2012 9th International Conference on Electrical Engineering, Computing Science and Automatic Control
Mexico City, Mexico. September 26-28, 2012

Stability Analysis and Experiments for a Force Augmenting Device

S. K. Gadi[1], R. Lozano[1,2], R. Garrido[1], A. Osorio[3]
[1] Department of Automatic Control, UMI LAFMIA CNRS-CINVESTAV, Av. IPN 2508. 07360 México D.F.
[2] Heudiasyc UMR-6599, CNRS-UTC, Compiegne, France
[3] CGSTIC - CINVESTAV Av. IPN 2508. 07360 México D.F.

***Abstract*— We present preliminary results of a one degree of freedom (DOF) linear moving force augmenting device (FAD) with a force sensor for enhancing the lifting capabilities of a human user. We perform a stability test of the feedback loop formed by the device and a model of the human operator. It is shown that the operator lifts a small fraction of the total weight of the load. The proposed control scheme is illustrated using numerical simulations and an experiment.**

Keywords: Exoskeleton, force augmenting device, load handling.

I. Introduction

Recently, there has been a lot of interest in developing exoskeletons and force augmenting devices, i.e. mechanical systems that are worn by humans in such a way as to increase their force. There exist many possible applications for these devices; for instance, in industries where it is commonly required to move heavy loads. This task is mostly done by machines which are usually controlled by humans who do not necessarily feel the force exerted on the load. This may lead to unsafe conditions in confined spaces with obstacles. Exoskeletons represent a possible solution to this problem [1]. Indeed, a force augmenting device amplifies the human strength and allows the operator to handle heavy loads but still feeling the effort performed to move the load [2].

Hardiman is one of the first exoskeletons which was based on master slave considerations [3], [4]. Electromyography (EMG) and force sensors are commonly used to obtain information of the human interaction force. The HAL exoskeleton is one of the successful exoskeletons with EMG sensing [5], [6]. Disabled, elderly and injured persons can use the exoskeletons based on EMG sensors [7]. Devices based on EMG have limitations since the signals measured using surface electrodes are weak and noisy; these signals also change with the user [8] and the number of repetitions of the task [9]. Furthermore, these devices need longer training periods [10]. Algorithms such as sensitivity amplification control (SAC) [11], [12] do not need any sensors but require an accurate knowledge of the exoskeleton's mathematical model. In [13] it is shown that knowledge of the system model is not required when the inverse dynamic model is replaced by a neural model.

In this paper, we present a one degree of freedom (DOF) linearly moving force augmenting device (FAD) with a force sensor for enhancing the lifting capabilities of a human user. The two main objectives of the control algorithm presented in this paper are the following:

1) The user should always feel a fraction of the load he is handling. In this regard, note that in [14], [15], the user feels the load only while the user wishes to change position.
2) The load should slowly return to the initial position when the user stops interacting with the load.

This paper is organized as follows: Section II presents the mechanical setup of a FAD, which is considered for the demonstration of the control algorithm. The dynamical model of the FAD is described in Section III while a model of a human operator is given in section IV. The control algorithm is proposed in Section V. The stability analysis of the closed-loop system is presented in Section VI and the performance analysis is given in Section VII. An illustrative example is described in Section VIII and an experimental result is shown in Section IX. Concluding remarks are finally given in Section X.

II. Mechanical Setup

Fig. 1 depicts a sketch of the force augmenting device and Fig. 2 is a photograph of it. It consists of a mechanical block of mass (M) connected to an electric motor via a ball screw mechanism. The ball screw mechanism converts the rotational force (torque, τ) developed by the motor to a linear force (F_m) which moves the mechanical block.

The position of the mechanical block is considered to be zero when the block is in contact with the lower limit of the mechanical travel of the ball-screw mechanism and positive when the block is above that level. An encoder attached to the motor allows measuring indirectly the block position y_e.

III. Modeling of the force augmenting device

Consider Fig. 1, the driving force (F_m) of a ball-screw mechanism is proportional to the torque output of the electric motor (τ) [16], [17], we can write

$$F_m = K_m \tau \quad (1)$$

IEEE Catalog Number: CFP12827-CDR
ISBN: 978-1-4673-2168-6
978-1-4673-2169-3/12/$31.00 ©2012 IEEE

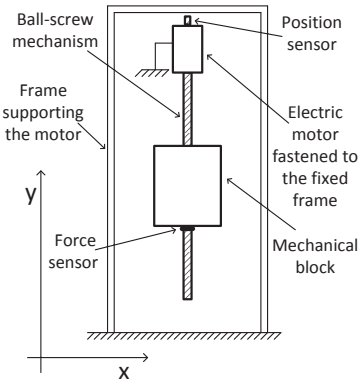

Fig. 1: Mechanical setup with a linear sliding mass with an actuator.

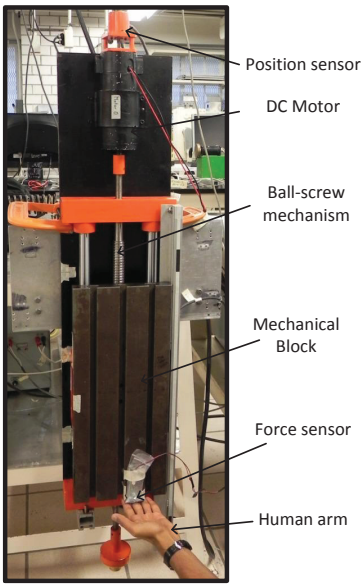

Fig. 2: User operating the moving block

where K_m is a positive constant.

Since the power amplifier of the motor is working in torque mode, its dynamics are fast (see Appendix). Ignoring these dynamics allows writing

$$\tau = K_T V \quad (2)$$

where K_T is a positive constant and V is the voltage input to the servomechanism.

Substituting (2) into (1), yields

$$F_m = K_m K_T V \quad (3)$$

Let M be the mass of the mechanical block and K_f a viscous friction coefficient. Therefore, the model of the mechanical block can be written as:

$$M\ddot{y}_e = -K_f \dot{y}_e + F \quad (4)$$
$$F = F_m + F_h - W \quad (5)$$

where $W = Mg$ is the weight of the mechanical block, F is the total force exerted on the mechanical block and F_h is the force exerted by the human. Assuming zero initial conditions, the following transfer function describes the dynamics from F to y_e

$$\frac{y_e(s)}{F(s)} = \frac{1}{Ms^2 + K_f s} \quad (6)$$

IV. Model of the human operator

In 1953 Merton proposed a servo model for generating movements in biological motor systems [18], [19], however the servo model was found to be wrong in experiments [19]. Improved versions of servo models like the α equilibrium-point model [20], [21], [19], the λ equilibrium-point model [22], [23], [19], and the unified equilibrium-point model were developed. The trajectory achieved by the human arm may be different from the reference trajectory due to the presence of external forces on the joint. Therefore the reference trajectory can be seen as a virtual trajectory [24], [25], [19]. These servo controls are hence known as virtual trajectory controls. Many human models are available like those based on virtual trajectory control and the inverse dynamics control [26], [27]. The most complete form of a human model is the enhanced equilibrium-point control model proposed in [19].

Fig. 3 shows a human operator model proposed in [19] with the addition of an external torque or reaction torque; the following equations describe this model.

$$y_v(s) = e_{pos}(s)G_{pos} + e_{vel}(s)G_{vel} + y_{vd}(s) \quad (7)$$
$$e_{pos}(s) = y_{vd}(s) - y_{hr}(s)e^{-sd_1} \quad (8)$$
$$e_{vel}(s) = y_{vd}(s)s - y_{hr}(s)se^{-sd_2} \quad (9)$$
$$Is^2 y_{hr}(s) = -Bsy_{hr}(s) + K(y_v(s) - y_{hr}(s)) + \tau_e(s) \quad (10)$$
$$\tau_e(s) = F_e(s)l_a \quad (11)$$
$$y_h(s) = y_{hr}(s)l_a \quad (12)$$

where $y_{hr}(s)$ is the human arm position in radians, $y_h(s)$ is the human arm position in meters, $y_v(s)$ is a control signal known as the virtual trajectory, I is the moment of inertia of the human arm, K is the muscle stiffness, B is the muscle viscosity, d_1 is a delay in the position feedback, d_2 is a delay in the velocity feedback, $y_{vd}(s)$ is the virtual desired position, l_a corresponds to the arm length, G_{pos} and G_{vel} are the proportional and derivative gains of the controller respectively.

Fig. 4 shows the human arm interaction with the FAD. The force exerted on the FAD by the human arm (F_h) is equal and opposite to the force exerted by the FAD on the human arm (F_e) [14], which can be given as [28]

$$F_h = -F_e = (y_h - y_e)E \quad (13)$$
$$\Rightarrow \tau_e = F_e l_a = (y_e - y_h)El_a \quad (14)$$

where E represents the physical compliance of the human flesh and the force sensors existing between the human

IEEE Catalog Number: CFP12827-CDR
ISBN: 978-1-4673-2168-6
978-1-4673-2169-3/12/$31.00 ©2012 IEEE

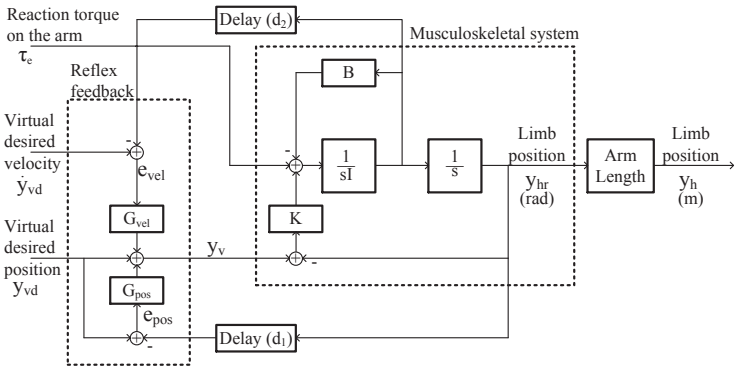

Fig. 3: Human model.

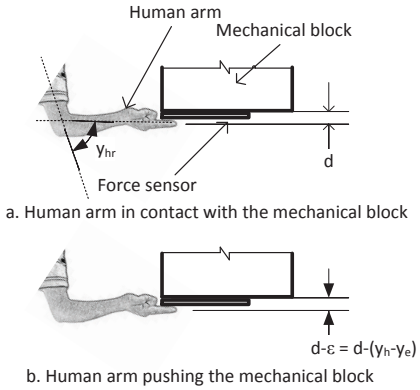

Fig. 4: The human arm interacting with the FAD.

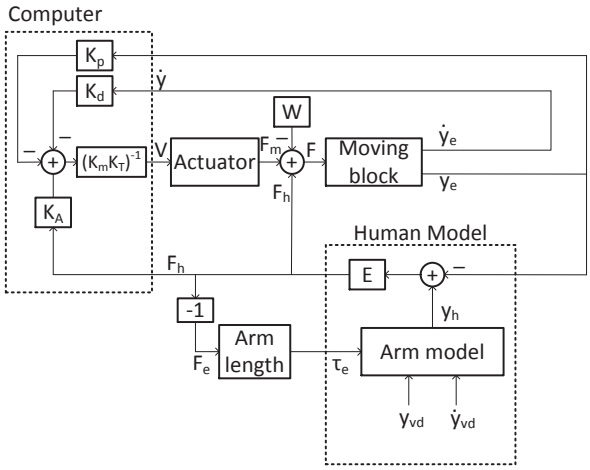

Fig. 5: Closed-loop control algorithm.

and the FAD. The stiffness of the force sensor is very high compared to the one of the human flesh, hence E can be considered as the flesh compliance [14]. The estimated value of E for a subject is 0.92 N/mm [28].

V. The Control Algorithm

The following control algorithm can be applied, as shown in Fig. 5.

$$F_m = K_A F_h - K_d \dot{y}_e - K_p y_e \quad (15)$$

where K_A is the amplification force gain, K_p is the proportional gain and $-K_d\dot{y}$ represents a velocity feedback that introduces damping into the system.

Substituting the control algorithm (13), and (15) into (4) yields

$$\begin{aligned} M\ddot{y}_e &= -W - (K_d + K_f)\dot{y}_e - K_p y_e + \\ &\quad (K_A + 1)F_h \quad (16) \\ \Rightarrow M\ddot{y}_e &= -W - (K_d + K_f)\dot{y}_e - K_p y_e + \\ &\quad (K_A + 1)E(y_h - y_e) \quad (17) \end{aligned}$$

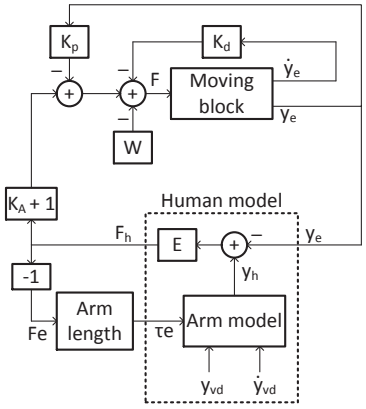

Fig. 6: Simplified form of the algorithm shown in Figure 5.

IEEE Catalog Number: CFP12827-CDR
ISBN: 978-1-4673-2168-6
978-1-4673-2169-3/12/$31.00 ©2012 IEEE

VI. Stability analysis

The closed loop system depicted in Fig. 5 can be simplified to the block diagram shown in Fig. 6.

Applying the Laplace transformation to (17), we get the following closed loop transfer function

$$\frac{y_e(s)}{y_h(s)} = \frac{(K_A+1)E}{Ms^2+(K_d+K_f)s+(K_p+E(K_A+1))} \quad (18)$$

Neglecting the delays d_1 and d_2 in the human model allows rewriting (7) - (11) in the frequency domain as

$$\begin{aligned} Is^2y_{hr}(s) &= y_{hr}(s)[-Bs-K-El_a^2- \\ &\quad KG_{vel}s-KG_{pos}]+y_{vd}(s)[KG_{vel}s+ \\ &\quad KG_{pos}+K]+y_e(s)[El_a] \end{aligned} \quad (19)$$

We will perform the stability test on the closed loop system by applying the Routh Hurwitz stability analysis. Substituting (12) and (18) into (19), we get

$$\frac{y_{hr}(s)}{y_{vd}(s)} := \frac{N_{hr}(s)}{D(s)} \quad (20)$$

$$\frac{y_e(s)}{y_{vd}(s)} := \frac{N_e(s)}{D(s)} \quad (21)$$

$$\begin{aligned} N_{hr}(s) &= ((G_{pos}+1)K+G_{vel}Ks)(Ms^2+ \\ &\quad (K_d+K_f)s+K_p+E(K_A+1)) \end{aligned} \quad (22)$$

$$N_e(s) = E(K_A+1)l_a((G_{pos}+1)K+G_{vel}Ks) \quad (23)$$

$$\begin{aligned} D(s) &:= a_4s^4+a_3s^3+a_2s^2+a_1s+a_0 \\ a_4 &= IM \\ a_3 &= BM+IK_d+IK_f+G_{vel}KM \\ a_2 &= EMl_a^2+BK_d+BK_f+EI+ \\ &\quad IK_p+KM+EIK_A+G_{vel}KK_d+ \\ &\quad G_{vel}KK_f+G_{pos}KM \\ a_1 &= BE+BK_p+KK_d+KK_f+BEK_A+ \\ &\quad EG_{vel}K+G_{pos}KK_d+G_{pos}KK_f+ \\ &\quad G_{vel}KK_p+EK_dl_a^2+EK_fl_a^2+ \\ &\quad EG_{vel}KK_A \\ a_0 &= EK_pl_a^2+EK+KK_p+ \\ &\quad EG_{pos}K+EKK_A+G_{pos}KK_p+ \\ &\quad EG_{pos}KK_A \end{aligned} \quad (24)$$

As per the Routh Hurwitz stability criterion, the system is stable if and only if following conditions are satisfied.

$$a_0>0;\ a_1>0;\ a_2>0;\ a_3>0;\ a_4>0$$

$$b_1 := \frac{a_3a_2-a_4a_1}{a_3} > 0 \quad (25)$$

$$c_1 := \frac{b_1a_1-a_3b_2}{b_1} > 0$$

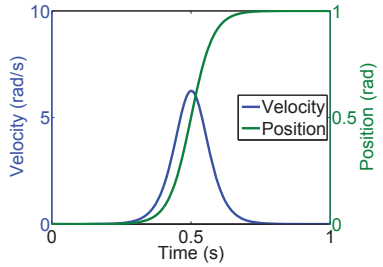

Fig. 7: An example of position and velocity trajectories of an arm

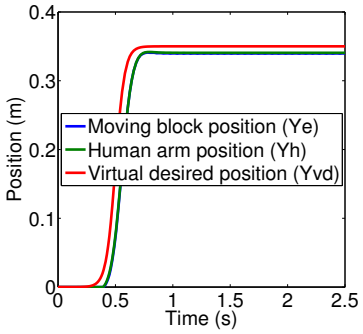

Fig. 8: Position vs Time

VII. Performance analysis

At equilibrium point, (16) can be simplified to

$$F_h = \frac{W+K_py_e}{(K_A+1)} \quad (26)$$

which highlights that the human always feels a relatively small portion of the weight.

When the operator releases his hand from the load, the system dynamics shown in (17) changes to

$$M\ddot{y}_e = -K_py_e-(K_d+K_f)\dot{y}_e-W \quad (27)$$

which is stable since K_p and K_d+K_f are positive. The position at the equilibrium point is:

$$y_e = -\frac{W}{K_p} \quad (28)$$

The above position is negative, however, the mechanical limit will prevent the block from moving below the ground level $y_e = 0$.

VIII. Simulation results

In this section, we will simulate a numerical example. An experiment has been conducted in [19] on an user's arm to estimate the parameters of inertia (I), stiffness (K) and viscosity (B), the delays were obtained from [29], [30]. Taking one of the set of values for human dynamics given in [19], yields $I = 0.1\frac{\text{Nm}}{\text{rad}\times\text{s}^2}$, $K = 4\frac{\text{N}}{\text{rad}}$, $B = 0.89\frac{\text{Nm}}{\text{rad}\times\text{s}}$, $G_{pos} = 2$, $d_1 = 0.04$s, $G_{vel} = 0.3$s and $d_2 = 0.04$s.

Considering a mechanical system with $M = 10$Kg, $K_b = 1\frac{\text{N}\times\text{s}}{\text{m}}$, $K_f = 0.5\frac{\text{N}}{\text{m}}$ and arm length of $35cm$,

IEEE Catalog Number: CFP12827-CDR
ISBN: 978-1-4673-2168-6
978-1-4673-2169-3/12/$31.00 ©2012 IEEE

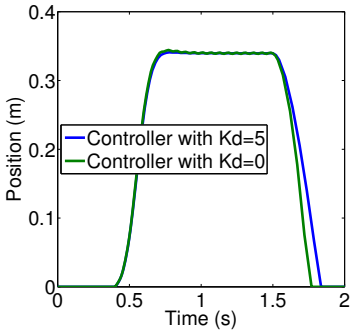

Fig. 9: Position trajectories of the moving block when the user releases his hand at $t = 1.5s$

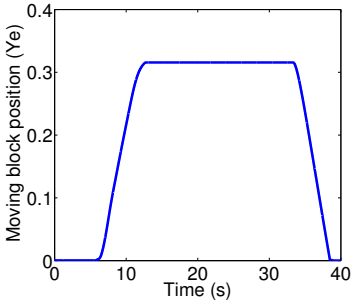

Fig. 10: Experimental result showing moving block position (y_e) vs time

$E = 0.92$ N/mm, $K_A = 10$, $K_p = 1$ and $K_d = 5$, we can get $a_0 = 1.2156 \times 10^5 > 0$, $a_1 = 2.1839 \times 10^4 > 0$, $a_2 = 2.2706 \times 10^3 > 0$, $a_3 = 21.45 > 0$, $a_4 = 1 > 0$, $b_1 = 1.2525 \times 10^3 > 0$, and $c_1 = 1.9757 \times 10^4 > 0$, which satisfy the conditions required for the stability as given in (25). Time vs position simulation result for the above given values is shown in Fig. 8. The position trajectories of the moving block while the hand is released are shown in Fig. 9.

The trajectories achieved by a human arm during point to point movement are usually straight with bell-shaped velocity profiles [31], that is why we use a sigmoid function as the desired input. An example of position and velocity trajectories of an arm movement are shown in Fig. 7.

IX. Experiment results

The experiment consists of lifting the block to a given position by pushing the force sensor upwards, then maintaining that position for a given period of time by exerting on the sensor a constant upwards force and then releasing the force sensor and observing the way the block returns to its equilibrium position on the lower limit of the mechanical travel of the ball-screw mechanism. The mechanical block position (y_e) vs time and the force exerted by human arm (F_h) vs time graphs of the experiment can be seen in Fig. 10 and Fig. 11 respectively.

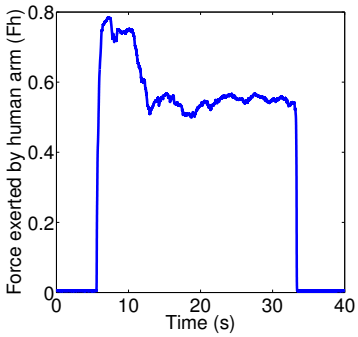

Fig. 11: Experimental result showing force exerted by human arm (F_h) vs time

X. Conclusion

In this paper we have presented a one degree of freedom (DOF) linearly moving force augmenting device. The prototype includes a force sensor, an electrical motor and a ball-screw mechanism so that it enhances the lifting capabilities of the operator. The conditions for the closed loop system stability were obtained by the Routh Hurwitz stability criterion.

We have tested the approach using numerical simulations and the performance of the strategy has been satisfactory. It must be pointed out that for the delays considered in the example, the performance of the control algorithm was satisfactory despite the fact that it was designed neglecting the delays of the human model.

Even though the algorithm proposed in this paper is simple to implement as compared to other existing algorithms, the experimental results were satisfactory. As can be seen in Fig. 11, the user exerts an upward force on the sensor while the block moves upwards or is held in a constant position. This was one of the objectives of the control scheme.

Appendix

An electric motor can be modeled as

$$\begin{aligned} \frac{\tau(s)}{V_m(s)} &= \frac{K_t(Js+B)}{L_mJs^2 + (L_mB + R_mJ)s + (K_eK_t + R_mB)} \\ \tau &= K_tI \end{aligned} \quad (29)$$

where τ is the shaft torque of the motor in newton meters, V_m is the voltage input to the motor in volts , K_t is motor torque constant in newton meters per ampere, J is inertia in N.m.s^2, B is friction in N.m.s, L_m is the inductance of the motor in Ω.s, $R_m = R_a + R_l$ is the motor resistance in Ω, K_e is the back emf constant of the motor V.s/rad and I is the motor current in amperes.

In the experimental setup, the motor is connected to an amplifier working in torque mode with current feedback as shown in Fig. 12. The closed loop system

$$\frac{\tau(s)}{V(s)} = K_tK_E \left[\frac{\left(K_p + \frac{K_I}{s}\right) K_A \frac{I(s)}{V_m(s)}}{1 + K_C \left(K_p + \frac{K_I}{s}\right) K_A \frac{I(s)}{V_m(s)}} \right] \quad (30)$$

IEEE Catalog Number: CFP12827-CDR
ISBN: 978-1-4673-2168-6
978-1-4673-2169-3/12/$31.00 ©2012 IEEE

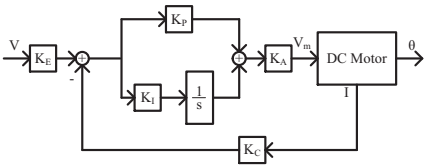

Fig. 12: DC motor with a power amplifier in current feedback mode

where V is the control input to the amplifier in volts, K_C is the current feedback gain in volt per ampere, K_A is the H Bridge gain of the amplifier, K_E is input gain of the amplifier and K_P and K_I are the proportional and integral gains, respectively for the PI controller within the amplifier. Selecting a larger value for K_I, we can simplify (30) as

$$\tau(s) = K_t K_E \left[\frac{1}{K_C}\right] V(s) = K_T V(s) \tag{31}$$

where $K_T = \frac{K_t K_E}{K_C}$.

Acknowledgements

The authors would like to thank Gerardo Castro, and Jesús Meza, for their help in electrical setup and Robrto Lagunes for his help with the mechanical setup.

References

[1] Wan soo Kim, Seung hoon Lee, Hee don Lee, Seung nam Yu, Jung soo Han, and Chang soo Han. Development of the heavy load transferring task oriented exoskeleton adapted by lower extremity using quasi - active joints. In *ICCAS-SICE, 2009*, pages 1353 –1358, aug. 2009.

[2] T.J. Snyder and H. Kazerooni. A novel material handling system. In *1996. Proceedings., 1996 IEEE International Conference on Robotics and Automation,*, volume 2, pages 1147 –1152 vol.2, apr 1996.

[3] K.E. Gilbert, P.C. Callan, and General Electric Co Schenectady NY Speciality Materials Handling Products Operation. *Hardiman I Prototype Project*. Defense Technical Information Center, 1968.

[4] BJ Makinson. Research and development prototype for machine augmentation of human strength and endurance. Hardiman I Project. Technical report, DTIC Document, 1971.

[5] S. Lee and Y. Sankai. Power assist control for leg with hal-3 based on virtual torque and impedance adjustment. In *2002 IEEE International Conference on Systems, Man and Cybernetics.*, volume 4, pages 6–pp. IEEE, 2002.

[6] K. Kasaoka and Y. Sankai. Predictive control estimating operator's intention for stepping-up motion by exoskeleton type power assist system hal. In *2011 IEEE/RSJ International Conference on Intelligent Robots and Systems, 2001. Proceedings.*, volume 3, pages 1578–1583. IEEE, 2001.

[7] K. Kiguchi, T. Tanaka, and T. Fukuda. Neuro-fuzzy control of a robotic exoskeleton with emg signals. *IEEE Transactions on Fuzzy Systems*, 12(4):481–490, 2004.

[8] Wendy M. Murray, Scott L. Delp, and Thomas S. Buchanan. Variation of muscle moment arms with elbow and forearm position. *Journal of Biomechanics*, 28:513–525, May 1995.

[9] P. Bonato, P. Boissy, U. Della Croce, and S.H. Roy. Changes in the surface emg signal and the biomechanics of motion during a repetitive lifting task. *IEEE Transactions on Neural Systems and Rehabilitation Engineering*, 10(1):38 –47, march 2002.

[10] E. Guizzo and H. Goldstein. The rise of the body bots [robotic exoskeletons]. *Spectrum, IEEE*, 42(10):50 – 56, oct. 2005.

[11] H. Kazerooni, J.-L. Racine, Lihua Huang, and R. Steger. On the control of the berkeley lower extremity exoskeleton (bleex). In *Proceedings of the 2005 IEEE International Conference on Robotics and Automation, 2005. ICRA 2005.*, pages 4353 – 4360, april 2005.

[12] Xiuxia Yang, Zhang Yi, Zhiyong Yang, Lihua Gui, and Wenjin Gu. Human-machine intelligent robot system control based on study algorithm. In *IEEE International Conference on Industrial Technology, 2008. ICIT 2008.*, pages 1 –6, april 2008.

[13] Z. Yang, L. Gui, X. Yang, and W. Gu. Simulation research of exoskeleton suit based on neural network sensitivity amplification control. In *Control and Decision Conference, 2008. CCDC 2008. Chinese*, pages 3340–3344. IEEE, 2008.

[14] H. Kazerooni. Human machine interaction via the transfer of power and information signals. *ASME Winter Annual Meeting*, December 1988.

[15] H. Kazerooni. Extender: a case study for human-robot interaction via transfer of power and information signals. In *1993. Proceedings., 2nd IEEE International Workshop on Robot and Human Communication*, pages 10 –20, nov 1993.

[16] Nook Industries Inc. Precision ball screw assembly technical introduction. *http://www.nookindustries.com/pdf/NookBallTechnical.pdf*, 2011.

[17] Techno Inc. Technical information. *http://www.techno-isel.com/Tic/H834/PDF/H834P011.pdf*, 2012.

[18] PA Merton. Speculations on the servo-control of movement. In *Ciba Foundation Symposium-The Spinal Cord*, pages 247–260. Wiley Online Library, 1953.

[19] J. McIntyre and E. Bizzi. Servo hypotheses for the biological control of movement. *Journal of Motor Behavior*, 25(3):193–202, 1993.

[20] P.M.H. Rack and DR Westbury. The effects of length and stimulus rate on tension in the isometric cat soleus muscle. *The Journal of Physiology*, 204(2):443–460, 1969.

[21] JA Hoffer, S. Andreassen, et al. Regulation of soleus muscle stiffness in premammillary cats: intrinsic and reflex components. *Journal of Neurophysiology*, 45(2):267–285, 1981.

[22] A.G. Feldman et al. Once more on the equilibrium-point hypothesis (lambda model) for motor control. *Journal of motor behavior*, 18(1):17, 1986.

[23] MB Berkinblit, AG Feldman, and OI Fukson. Adaptability of innate motor patterns and motor control mechanisms. *Behavioral and Brain Sciences*, 9(04):585–599, 1986.

[24] ML Latash and GL Gottlieb. Reconstruction of shifting elbow joint compliant characteristics during fast and slow movements. *Neuroscience*, 43(2-3):697–712, 1991.

[25] N. Hogan. An organizing principle for a class of voluntary movements. *The Journal of Neuroscience*, 4(11):2745–2754, 1984.

[26] Nicolas Schweighofer, Michael A. Arbib, and Mitsuo Kawato. Role of the cerebellum in reaching movements in humans. I. distributed inverse dynamics control. *European Journal of Neuroscience*, 10(1):86–94, 1998.

[27] N. Schweighofer, J. Spoelstra, M.A. Arbib, and M. Kawato. Role of the cerebellum in reaching movements in humans. II. a neural model of the intermediate cerebellum. *European Journal of Neuroscience*, 10(1):95–105, 1998.

[28] T.C. Pataky, M.L. Latash, and V.M. Zatsiorsky. Viscoelastic response of the finger pad to incremental tangential displacements. *Journal of biomechanics*, 38(7):1441–1449, 2005.

[29] J.R. Dufresne, J.F. Soechting, and C.A. Terzuolo. Electromyographic response to pseudo-random torque disturbances of human forearm position. *Neuroscience*, 3(12):1213 – 1226, 1978.

[30] J.R. Dufresneand J.F. Soechting and C.A. Terzuolo. Reflex motor output to torque pulses in man: identification of short- and long-latency loops with individual feedback parameters. *Neuroscience*, 4(10):1493–500, 1979.

[31] J. Randall Flanagan and David Ostry. Trajectories of human multi-joint arm movements: Evidence of joint level planning. In Vincent Hayward and Oussama Khatib, editors, *Experimental Robotics I*, volume 139 of *Lecture Notes in Control and Information Sciences*, pages 594–613. Springer Berlin / Heidelberg, 1990. 10.1007/BFb0042544.

IEEE Catalog Number: CFP12827-CDR
ISBN: 978-1-4673-2168-6
978-1-4673-2169-3/12/$31.00 ©2012 IEEE